Analytica Chimica Acta 1165 (2021) 338478

Contents lists available at ScienceDirect

Analytica Chimica Acta

journal homepage: www.elsevier.com/locate/aca

An exonuclease protection and CRISPR/Cas12a integrated biosensor for the turn-on detection of transcription factors in cancer cells

Bingzhi Li [b], Zicheng Shao [c], Yue Chen [a, *]

[a] School of Nursing, Nanjing Medical University, Nanjing, 211166, China
[b] School of Food Science and Pharmaceutical Engineering, Nanjing Normal University, Nanjing, 210023, China
[c] Department of Hepatobiliary Surgery, The Second Affiliated Hospital of Nantong University, Nantong, 226000, China

HIGHLIGHTS

- A CRISPR/Cas12a-based biosensor targeting TFs was developed.
- Exonuclease protection and Cas12a were integrated for TFs sensing.
- Convenient detection of NF-κB p50 with LOD of 0.2 pM was realized.
- This sensor can be applied in the screening and evaluation of TFs inhibitors.

GRAPHICAL ABSTRACT

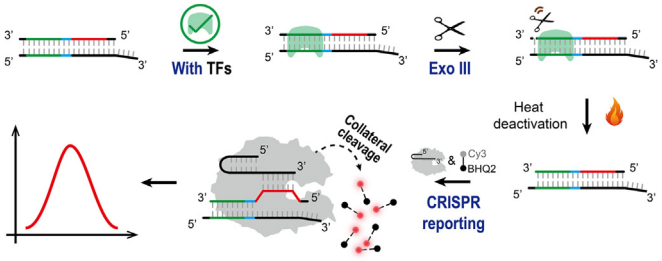

ARTICLE INFO

Article history:
Received 4 March 2021
Accepted 30 March 2021
Available online 4 April 2021

Keywords:
CRISPR
Transcription factor
DNA binding protein
Nuclear factor-kappa B
Functional nucleic acid
Exonuclease protection assay

ABSTRACT

Transcription factors (TFs) are critical proteins that regulate the expression of genes, and the abnormal change of TFs levels is directly related to physical dysfunctions. Herein, we developed a clustered regularly interspaced short palindromic repeats (CRISPR)-based biosensor for the measurement of TFs level with the assistance of exonuclease protection assay. A dsDNA (activator) with the ability to activate Cas12a was engineered to contain TFs binding domain, and the binding between TFs and the activator can protect the dsDNA from being digested by exonuclease III (Exo III). The reserved activator then triggered a CRISPR/Cas12a reporting reaction to produce fluorescent signal for detection. In the detection of nuclear factor-kappa B (NF-κB) p50 subunit, the limit of detection of 0.2 pM and limit of quantification of 0.6 pM were obtained respectively, and the performance of this biosensor has been challenged by cell nucleoprotein extracts. Additionally, this method can be applied in the screening and evaluation of TFs inhibitors, calculating the IC50 of oridonin. Integrating merits including high sensitivity, low cost, and good portability, this method may enrich the arsenal for TFs-related applications.

1. Introduction

The *in vivo* activity of transcription factors (TFs) is to regulate transcription via associating with specific domains in genes [1,2], which is based on the recognition and binding between TFs and their binding sites [3,4]. The TFs-DNA binding is a critical event in cell signaling because it collects the information from signaling pathways, initiates the expression of proteins, and makes cells respond to various stimuli [1]. Therefore, the abnormal change of TFs level can lead to the alteration of cell patterns, which is typically related to pathological events [5]. The dysregulation of TFs levels is derived from the variation of genes decoding TFs, the disturbance

* Corresponding author.
E-mail address: chenyue1005@njmu.edu.cn (Y. Chen).

https://doi.org/10.1016/j.aca.2021.338478
0003-2670/

of signaling pathways, and irregular TFs translocation, thus accumulating evidence has indicated that there is a tight connection between TFs dysregulation and human diseases [6]. Nuclear factor-kappa B (NF-κB), a ubiquitous TF in the mammalian cell [7], regulates the expression of more than 150 genes and participates in the responses to inflammation stress [8], virus infections [9], cell proliferation [10], and apoptosis [11,12]. The change of NF-κB level is severely implicated in rheumatoid arthritis [13], cancer [14,15], and neurodegenerative disorders [16], which makes it a highly potential biomarker in the clinical diagnosis and treatment [6,17,18].

For the determination of TFs levels, the golden method is the electrophoretic mobility shift assay (EMSA); however, it is complicated and time-consuming because of the involvement of gel electrophoresis and the consumption of radioisotopes. Immunoassays are also applied in the detection of TFs, for example, Western blot (WB) and enzyme-linked immunosorbent assay (ELISA). Whereas, these assays are labor-intensive and hard to distinguish TFs from their precursors that share similar structures [19]. Recently, simplified and high-performance TFs assays have been developed, which promote the update of TFs assays [20]. Methods adopted fluorescent [21], colorimetric [22], electrochemical [23], and Raman [24] readout have been developed, while the fluorescent method is the most widely used one because of the integration of high sensitivity, environmentally friendly, and high portability. The most important step in the fluorescent sensing of TFs is to convert the binding signal between TFs and DNA domains into readable readout, which typically involves nucleic acid reaction networks [17]. For example, the Zhang group developed a sensing system based on exonuclease-protection and isothermal amplification, which realized the quantification of endogenous NF-κB p50 in cell extracts [21]. Our group has developed series of fluorescent TFs sensors based on enzyme-driven and conformational-change strategies [25–28]. Although high sensitivity down to femto-molar level was achieved, compromises in operational convenience have also been adopted. The hybridization of DNA segments and the assembly of highly-ordered DNA nanostructures requires delicately-controlled conditions and experiences in harness DNA operations. Therefore, it is highly desirable to develop robust fluorescent TFs assays with high sensitivity and selectivity.

Clustered regularly interspaced short palindromic repeats (CRISPR) are an adaptive immune system of prokaryotic organisms to prevent the invasion of viruses and bacteriophages [29]. The function of CRISPR relies on CRISPR-associated enzymes (Cas), which can assemble with RNA to realize the recognition and cleavage of specific nucleic acids. The CRISPR/Cas system has revolutionized gene editing because of its high efficiency in targeting genes of interest, and E. Charpentier and J. A. Doudna have been awarded the 2020 Nobel Prize in Chemistry because of their contributions in CRISPR/Cas-based gene editing. Beyond this, emerging reports have revealed that the CRISPR/Cas technology can be applied in the field of analytical chemistry. Zhang group has utilized RNA-guided Cas13a to realize the recognition of RNA, and the recognition can trigger the activation of Cas13a to cleave the collateral nucleic acid reporters to generate detectable fluorescent signals [30]. The RNA-guided DNA-targeting Cas12a has also been applied in the sensing of nucleic acids with the assistance of DNA reporters. Currently, the CRISPR/Cas-based analytical methods are developing rapidly [31–33]; however, its application scope is more focused on the analysis of nucleic acids, and it cannot be ignored that most of the meaningful analytes are in the form of non-nucleic-acid analytes. Although few investigations have applied the CRISPR/Cas-based sensor to the detection of non-nucleic-acid targets [34–36], further explorations for more strategies are still highly desirable.

Herein, we developed a CRISPR/Cas12a-based sensor for the detection of TFs by integrating exonuclease protection assay and CRISPR/Cas technology. The binding between TFs and their binding domains protects a dsDNA probe (referred to as the activator) from being digested by exonuclease III (Exo III). The reserved activator then functions as a signaling molecule to activate the Cas12a-crRNA complex, generating non-specific ssDNA cleavage activity to digest nearby the ssDNA. Using ssDNA labeled by fluorescent and quenching molecules at two termini as a reporter, the activation of Cas12a was recorded by fluorescent measurement. Following this sensing profile, the concentration of TFs was determined in a turn-on manner, and we demonstrated its applications in the real-sample analysis and the screening of TFs inhibitors. To the best of our knowledge, this is the first attempt to utilize CRISPR technology to report the DNA signal after exonuclease protection assay in TFs, and also a pioneering investigation in sensing critical TFs with CRISPR technology.

2. Methods and materials

2.1. Materials

All the HPLC-purified DNA sequences were supplied by Sangon Biotech (Shanghai, China), and their sequences are listed in Table S1. The buffers were prepared with molecular biology grade reagents (BBI, Shanghai, China). Human recombinant NF-κB p50 (41 kDa) was purchased from Enzo Life Sciences (NY, U.S.A). EnGen®Lba Cas12a and NEBuffer 2.1 were obtained from New England Biolabs (MA, U.S.A.). Human serum albumin (HSA) and bovine serum albumin (BSA) were purchased from BBI. Human interferon-gamma (IFN-γ) and oridonin (CAS No. 28957-04-2) was purchased from MedChemExpress (NJ, U.S.A.). DEPC-treated water supplied by Sangon Biotech was used throughout this research.

2.2. Cell culture and in vivo xenograft experiment

Human colon cancer DLD-1 cells were obtained from the American Type Culture Collection and maintained in RPMI-1640 with 10% fetal bovine (BBI) and cultivated with 5% CO_2 at 37 °C.

2.3. Extraction of nucleoproteins from real samples

Nucleoproteins were extracted from harvested cells using the nucleoprotein extraction kit obtained from Sangon Biotech. A BCA-based protein quantification kit (BBI) was used to unify the total protein concentration of all samples before further analysis.

2.4. ELISA kits

The ELISA quantification kit for NF-κB p50 was supplied by Biomatik (Ontario, Canada). The protein concentration of samples was quantified and unified with the Bradford protein assay (Sangon) before analyzing according to optical density following the manufacturer's protocols.

2.5. Protocols for the detection of NF-κB p50

According to the manufacturer's instructions, Engen® LbCas12a (50 nM, 20 μL) and the crRNA (500 nM, 2 μL) were mixed in 10 × NEBuffer® 2.1. Then, the FL-reporter (10 μM) was added to the solution and mixed in an ice bath. This solution is referred to as the CRISPR reporting mix (CRM), where the final concentrations of Cas12a-crRNA and FL-reporter are 10 nM and 1 μM, respectively.

For the detection of NF-κB p50, 15 μL of binding buffer (10 mM Na_2HPO_4/NaH_2PO_4, 100 mM CH_3COONa, 10 mM $Mg(CH_3COOH)_2$,

10% glycerol, 0.05 mg/mL poly (dI-dC) (Thermo Scientific, U.S.A.), pH = 7.2)) was mixed with 5 μL of activator (50 nM). Then, 30 μL of testing samples were added into the mixture and incubated at 37 °C for TFs-DNA binding. After binding for 15 min, Exo III was added into the solution, and ca. 2 unit/μL of Exo III and 2.5 nM of activator were incubated for 30 min at 37 °C, followed by heat deactivation at 65 °C. Then, 50 μL of CRM was introduced into the system. After keeping at 37 °C for 30 min, the Cas12a was heat deactivated at 65 °C for 10 min. The fluorescence was measured by a Biotek Synergy H1 (U.S.A.) plate reader (λ_{ex} = 510 nm, λ_{em} = 566 nm, 25 reads per well, gain = 100, measured from the top). The inhibition assay was conducted with similar procedures, except that 30 μL of a mixture containing 1 nM of NF-κB p50 and various concentrations of oridonin were added as the testing sample.

3. Results and discussion

3.1. The principle of this sensing system

The sensing mechanism of this biosensor is illustrated in Scheme 1. TFs have an intrinsic high affinity to specific DNA domains; thus, it is widely adopted to utilize consensus DNA domains to realize the recognition of specific TFs [37,38]. For example, NF-κB p50 shows a high affinity to dsDNA hybridized by 5′-GGGACTTTCC-3′ and its complementary sequence [22]. This domain was embedded into a dsDNA (referred to as the activator) for the binding of NF-κB p50 (indicated in green color). The NF-κB p50 binds to the recognition domain to form a stable protein-DNA complex, and then, Exo III which is a nuclease that can remove nucleotides of dsDNA in the 3′ to 5′ direction [39], was added to the system. The enzymatic activity of Exo III is specific for the blunt end and 5′-overhang end, so the Exo III can only digest the DNA probe from the 3′ termini of the upper strand. Whereas, when the Exo III encounter the binding spot of NF-κB p50 and the recognition domain, the steric hindrance derived from the huge size of NF-κB p50 would inhibit the progressive digestion of Exo III, resulting in the protection of dsDNA [39,40]. Afterward, the system is heat deactivated to make the TFs dissolve from the activator. In the following step, the CRM composed of Cas12a, crRNA, and FL-reporter was added into the solution. Because the activator contains the PAM domain (denoted in blue color) and a crRNA-recognizable domain, it can function as the activator to unleash

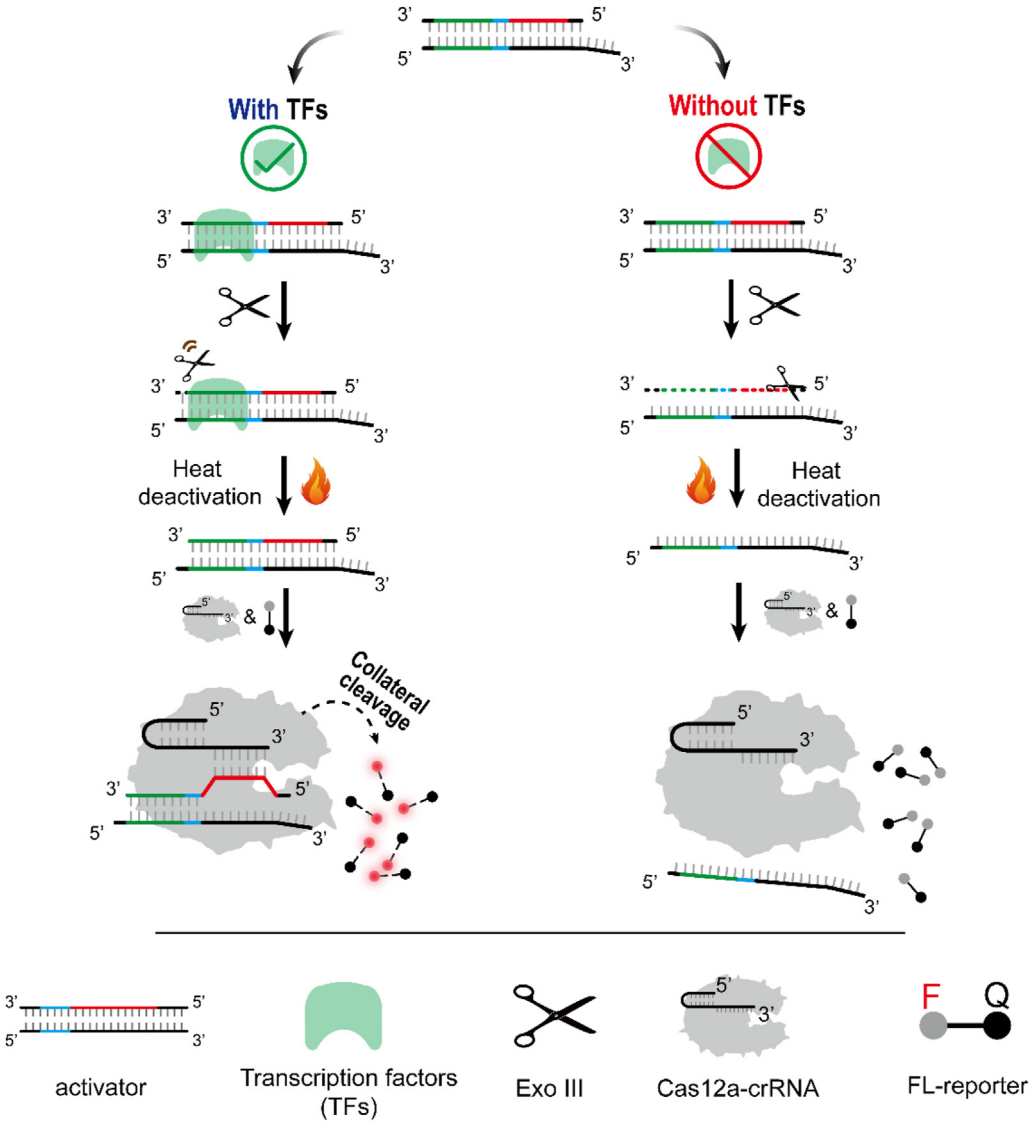

Scheme 1. The sensing mechanism of this method.

the ssDNA cleavage activity of Cas12a [41]. When the Cas12a possesses this activity, it would rapidly cleave the collateral FL-reporter, separating the 5′-Cy3 (fluorophore) and 3′-BHQ2 (quencher), resulting in an enhanced signal at the emission channel of Cy3 for quantification. Conversely, when no NF-κB p50 is in the solution, the Exo III successively digests the upper strand of the activator, leaving the below strand and causing no activation of Cas12a. On this occasion, the FL-reporter remains intact, so no detectable fluorescent feedback will occur. According to this sensing profile, the more NF-κB p50 is in the system, the higher emission will be recorded, forming a turn-on fluorometric biosensor for the detection of NF-κB p50 based on *in vitro* CRISPR technology.

3.2. Verification and optimization of this method

To verify the design of this sensor, we conducted a fluorescent scan in the first place, and the results are shown in Fig. 1a. It can be found that the mixture of the activator and the CRM exhibited high fluorescence at 566 nm, which is the result of the activation of Cas12a and the subsequent cleavage of the FL-reporter. While the sample prepared by mixing the activator with Exo III followed by the addition of CRM showed low fluorescence, which indicates that the Exo III digestion made the activator lost the ability to activate the Cas12a. However, when mixing the activator with the NF-κB p50 first, followed by Exo III digestion and CRISPR reporting in sequence, high fluorescence emission can be recorded. The results demonstrated that the digestion of Exo III made the activator lose the ability to activate the Cas12a, while the NF-κB p50 can protect the activator from losing this ability. The fluorescent spectra of the samples verified the biosensor we designed.

The sensing conditions were optimized to obtain improved performance. We optimized the conditions of Exo III digestion first, and Fig. 1b shows that when no NF-κB p50 was added in the system, 2 unit/μL of Exo III can make sufficient digestion to make the remaining activator lacks the ability to activate the Cas12a. Although this amount of Exo III cannot digest all the activator in the solution according to the digestion rate of Exo III [42], they could have conducted sufficient cleavage to impair the PAM sequence, thus making the remaining activator cannot induce significant fluorescence enhancement.

The conditions for CRISPR reporting was subsequently optimized. The activator was incubated with the CRM under different solutions, including ultrapure water, phosphate buffer, and a serial of widely used commercial buffers in molecular biology (NEBuffer 1.1, 2.1, and 3.1). The compositions of each buffer were listed in Table S2, and it was found that the highest fluorescence enhancement was obtained in NEBuffer 2.1, which could be derived from the suitable pH and ionic strength (Fig. 1C). It has been reported that the BSA can function as the stabilizer of plenty of enzymes and proteins [43,44]; thus, we deleted the BSA in the composition of NEBuffer 2.1 and found that the signal obtained in NEBuffer 2.1(BSA-) was significantly lower than that in NEBuffer 2.1 (Fig. S1), which indicated the role of BSA in enhancing the sensing. Previous reports indicated that the concentration of Mg^{2+} plays important role in accelerating the *trans*-cleavage of Cas12a [45]; thus, we

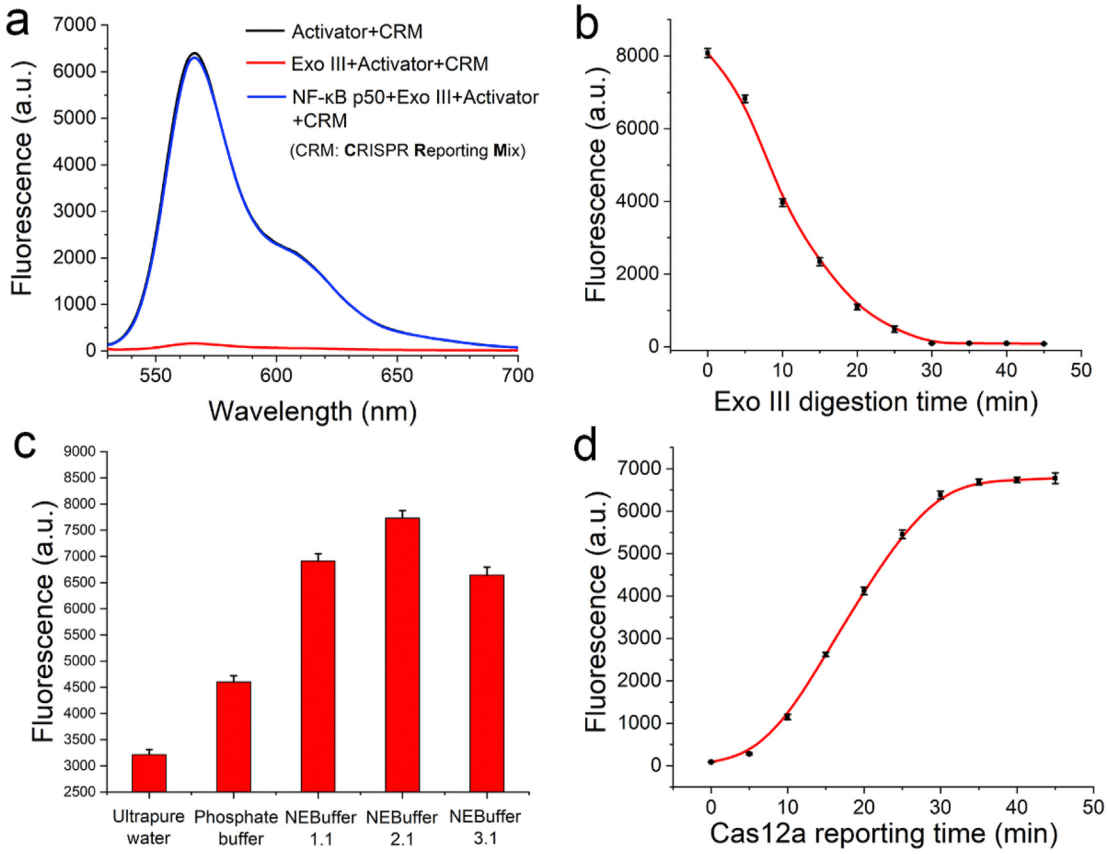

Fig. 1. The verification and optimization of this method. (a) The fluorescent spectra of samples in different conditions. (b) The optimization of Exo III digestion time. The final concentrations of the activator and Exo III were 2.5 nM and 2 unit/μL, respectively. (c) The optimization of CRISPR reporting reaction. In this experiment, 50 μL of CRM was mixed with the activator (5 nM, 50 μL). (d) The optimization of CRISPR reporting time. The activator (5 nM, 50 μL) was mixed 50 μL of CRM in NEBuffer 2.1, followed by fluorescence measurement at different times. Error bars indicate the standard deviation of three replicate determinations.

papared NEBuffer 2.1 with different Mg^{2+} concentrations and tested the signal response in these buffers. As shown in Fig. S2, signal intensified with the increased concentrations of Mg^{2+}, and the highest signal was obtained when the concentration of Mg^{2+} was 10 mM, which is the amount originally contained in NEBuffer 2.1. Following the protocol from previous reports and manufacturer's protocols [46], the incubation temperature was set at 37 °C. The kinetics of fluorescence change was recorded, and it was found that the fluorescence climbed and reached a plateau after 35 min of isothermal reaction (Fig. 1d).

3.3. Analytical performance of this biosensor

After optimizing the sensing conditions, the analytical performance of this biosensor was investigated. As illustrated in Fig. 2a, the sensing procedures include sample addition and incubation at a constant temperature, and all the processes are conducted in a single tube. Fig. 2b shows that the fluorescence of the system intensified with the increased concentrations of NF-κB p50, which revealed that this system can realize the turn-on fluorescent sensing of NF-κB p50 as expected. By plotting the concentrations of analyte (NF-κB p50) against the fluorescent intensity, a good linear relationship is established in the range of 0.5–1600 pM. The linear relationship levels off at high NF-κB p50 concentrations, which could be derived from the limited amount of FL-reporter. The limit of detection (LOD) and limit of quantification (LOQ) of this sensor targeting NF-κB p50 was determined as 0.2 pM and 0.6 pM according to the rules of S/N = 3 and S/N = 10, respectively (the calculations were detailed in Supplementary Materials). Table 1 listed the analytical performance of previously reported sensors targeting NF-κB p50 as well as that of this work, and it can be found that the low LOD and wide linear range makes this work quite outstanding, especially considering that this work contained no complicated nucleic acid reaction circuit for signal amplifications.

The selectivity of this sensor was challenged by a wide range of biomolecules, including nucleases, other TFs, and high-abundance ingredients contained in nucleoprotein extracts. The concentrations of the interferent were set 10-fold higher than that of NF-κB p50 (10 nM vs. 1 nM). As shown in Fig. 2d, only the sample added with NF-κB p50 exhibited high fluorescence, which indicated the selectivity of this sensor targeting NF-κB p50. The high selectivity was derived from both the specific recognition between NF-κB p50 and the activator, as well as the specific hybridization between crRNA and the activator.

The performance of this biosensor was investigated using nucleoprotein extracted from human colorectal cancer DLD-1 cells. It has been reported that the abnormal activation of the NF-κB pathway is ubiquitous in cancer cells, and the upregulation of NF-κB proteins in colorectal cancer cells is an important indicator for both diagnosis and treatment [15,54,55]. The nucleoprotein extracts were diluted by 10 times using the reaction buffer, then examined by this sensing system. The fluorescence signal for each detection was substituted into the regression curve presented in Fig. 2c to give a value of concentration for quantification. As shown in Table 2, our assay gave a detection result of 102.3 pM when no external NF-κB p50 was added, which implied that this sample could contain 102.3 pM of NF-κB p50 originally. To test the accuracy of this result, we subsequently conducted a spiking test and

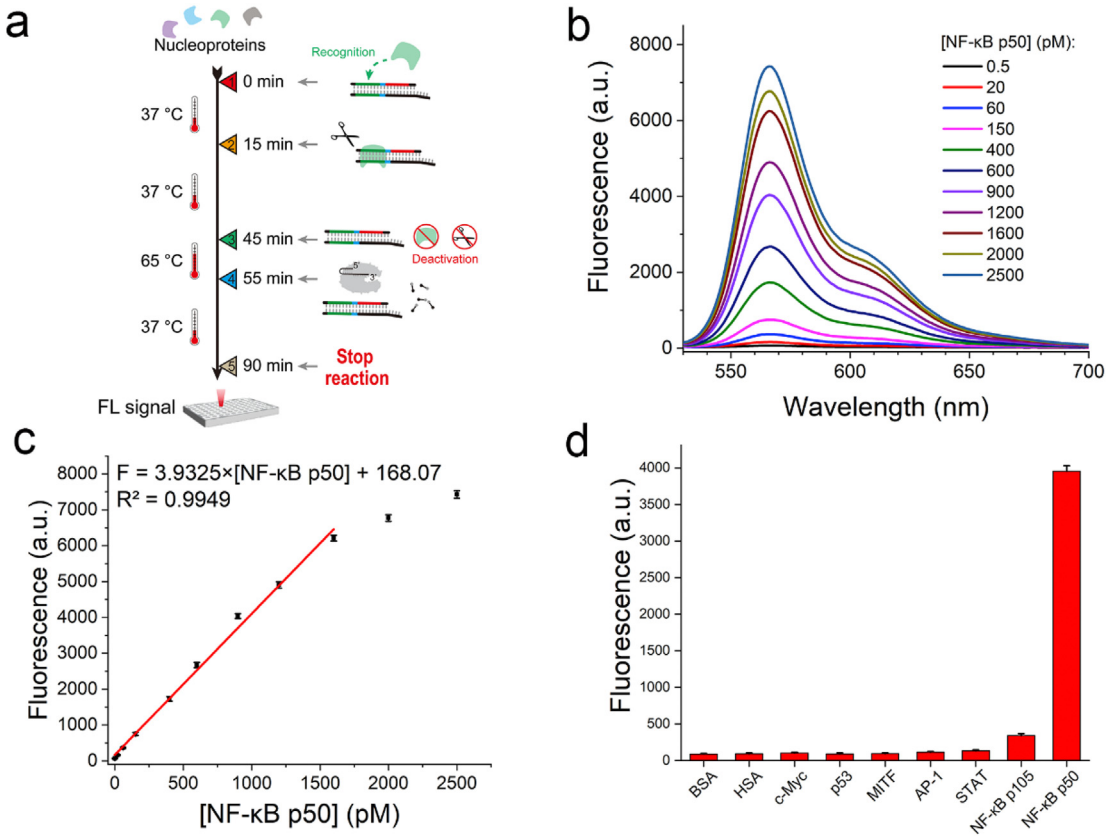

Fig. 2. The analytical performance of this method. (a) The workflow of this method. (b) The fluorescent spectra of the sensing system upon the addition of different concentrations of NF-κB p50. (c) The linear relationship between the concentrations of NF-κB p50 and the fluorescence intensity of the system. (d) The fluorescence intensity of the system with the addition of different targets. The tests were conducted according to the protocols described in the Experimental section, and error bars indicate the standard deviation of three replicate measurements.

Table 1
A comparison between this work and recently published investigation on the detection of NF-κB p50.

Signal forms	Amplification strategies	Linear range (nM)	Detection Limit (nM)	Ref.
Electrochemical	Exo III-added signal amplification	0.01–5	0.01	[47]
Fluorescent	Nb.*Bbv*CI-assisted signal amplification	0–50	2.2×10^{-3}	[48]
Fluorescent	Cascade signal amplification	3.8×10^{-4} - 15	2×10^{-4}	[49]
Fluorescent	DNAzyme-involved signal amplification	1×10^{-3} - 1	6.2×10^{-3}	[50]
Fluorescent	Rolling circle amplification	Not given	1.4×10^{-4}	[19]
Chemiluminescent	Isothermal exponential Amplification	1×10^{-5} - 1	6.23×10^{-6}	[51]
Colorimetric	Isothermal exponential Amplification	3×10^{-3} - 2	3.8×10^{-3}	[40]
Fluorescent	No amplification	0.5–50	0.2	[52]
Fluorescent	No amplification	1–50	1	[53]
Fluorescent	No amplification	0.05–5	0.0027	[46]
Fluorescent	**No amplification**	**$5 \times 10^{-4} - 1.6$**	**2×10^{-4}**	**This work**

Table 2
The calculation of recovery by spiking NF-κB p50 to DLD-1 nucleoproteins samples.

Sample	Content (pM)	Spiked (pM)	Found (pM)	Recovery[a] (%)	RSD (n = 6, %)
DLD-1 cells	102.3	50	148.7	92.8	3.1
		100	200.4	98.1	2.9
		150	248.2	97.3	3.4
		200	309.5	103.6	3.0

[a] Recovery: calculated by Recovery = ([Found] - [Content])/[Spiked] × 100%.

checked the result with commercialized ELISA kits. The sample was spiked with various concentrations of NF-κB p50, and the value of recovery ranged from 92.8 to 103.6%, which demonstrated that the linear relationship obtained in the buffer can be applied in the detection of a target in 10-fold diluted nucleoproteins. Meanwhile, the RSD obtained from 6 repetitive tests distributed in the range of 2.9%–3.4%, which indicated that this method can be applied in the real sample analysis with high precision. Fig. S3 shows the quantification results obtained from this assay and ELISA kits are in line with each other, which revealed the potential of this sensor in clinical applications. The average cost of the ELISA test is $ 7/test, which is 11 times higher than this method ($ 0.602, detailed in Table S3). Besides, different from ELISA which suffers from low precision because of the instability of antibodies and the reporting enzymes, CRISPR reporting elements (Cas enzymes, crRNA, reporting DNA) can be freeze-dried and stored for a long period, which has been applied in the on-site monitoring of virus including COVID-19 [56]. Our test showed that the sensing element can be stored at −20 °C for at least 2 months without significant loss of sensing performance (Table S4), considering its facile procedure including isothermal incubation and single-tube requirement, we believe that it could greatly serve the need for TFs detection at less-equipped scenarios.

3.4. Inhibition assay

It has been established that the abnormal upregulation of TFs is tightly correlated with the diseases including cancer, autoimmune, and inflammatory diseases, thus the inhibition of the overexpressed TFs is a critical strategy in drug development [57]. For example, mounting evidence has demonstrated that the constitutive activation of NF-κB was common in most cancers, and the block of NF-κB signaling could cause increased apoptosis of cancer cells [8,58]. Therefore, it is critical of developing convenient ways for the screening and evaluation of chemicals with inhibitory effects on TFs. Oridonin is a natural product obtained from *Rabdosia rubescens* that can inhibit the DNA binding of NF-κB p50 [59,60], and we used it as a model chemical to test the potential of our method in drug development. Different concentrations of oridonin were incubated with the same amount of NF-κB p50, and then the samples were subjected to our method. The fluorescence was plotted against the concentrations of oridonin (Fig. 3), and it can be found that the fluorescence decreased along with the increased concentrations of oridonin. We have also conducted a set of control experiments to examine that whether oridonin could directly interfere with the sensing process in the absence of NF-κB p50, and the results indicated that no significant fluorescence change was observed when 0–16 μM of oridonin was added to the reaction (Fig. S4). These results demonstrated that the oridonin caused the fluorescence change via inhibiting the binding between NF-κB p50 and DNA. When more oridonin was added, more binding was inhibited, thus more dsDNA was digested by Exo III to lose their ability to activate Cas12a. By fitting the data in Fig. 3, the half-maximal inhibition concentration (IC_{50}) of oridonin towards NF-κB p50 was calculated to be 3.37 μM. These results demonstrated that our method can be applied in assessing the inhibitory effect of chemicals on TFs.

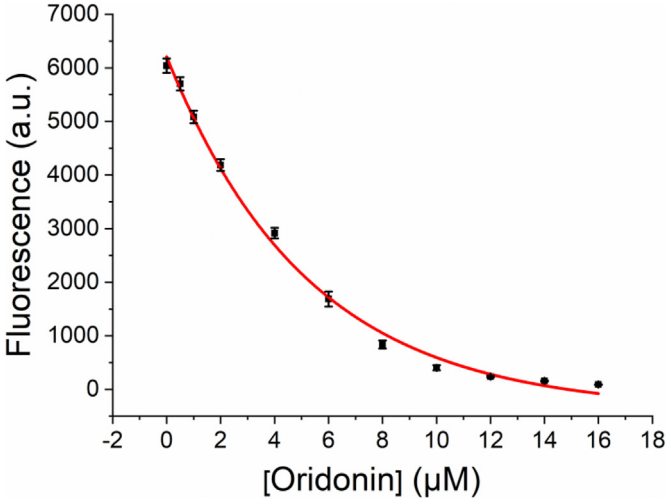

Fig. 3. The relationship between the concentration of oridonin and the fluorescence of the sensing system. Different concentrations of oridonin were mixed with 1 nM of NF-κB p50, followed by analysis as described in the Experimental Section.

4. Conclusion

In this study, the Exo III protection assay and CRISPR reporting system were combined to accomplish the sensing of TFs. The TFs can protect the activator from being digested by Exo III, thereby transducing the signal of TFs binding to nucleic acid signal. Then, the remaining activator after Exo III digestion activate the collateral cleavage of Cas12a effector, cleaving DNA reporter to generate significant fluorescence enhancement. Conversely, when there is no TFs in the system, the activator will be digested, resulting in no activation of Cas12a and no fluorescence enhancement. The sensing system can realize the sensitive and selective detection of NF-κB p50 with LOD of 0.2 pM, and it can be applied in specifically detecting NF-κB p50 in cell nucleoprotein extracts. Furthermore, we revealed the potential of this method in the evaluation of inhibitory effects of drugs towards TFs, which may greatly aid TFs-related biomedical research. In summary, this work developed a signal amplified sensing system for TFs quantification based on CRISPR/Cas12a, which enriched the application scope of CRISPR/Cas-enabled biosensing and the arsenal of TFs detection.

Declaration of competing interest

The authors declare that they have no known competing financial interests or personal relationships that could have appeared to influence the work reported in this paper.

Acknowledgments

This work was supported by grants from the Natural Science Foundation of Jiangsu Province (No. BK20200718), the Natural Science Foundation of the Jiangsu Higher Education Institutions of China (20KJB350010), the S&T Development Foundation of Nanjing Medical University (NMUB2020036), and the Scientific Research Start-Up Funding for Nanjing Normal University Introduced Talents (184080H202B246).

Appendix A. Supplementary data

Supplementary data to this article can be found online at https://doi.org/10.1016/j.aca.2021.338478.

References

[1] S.A. Lambert, A. Jolma, L.F. Campitelli, P.K. Das, Y. Yin, M. Albu, X. Chen, J. Taipale, T.R. Hughes, M.T. Weirauch, The human transcription factors, Cell 4 (2018) 650–665.
[2] K. Takahashi, S. Yamanaka, A decade of transcription factor-mediated reprogramming to pluripotency, Nat. Rev. Mol. Cell Biol. 3 (2016) 183–193.
[3] X. Li, J. Yang, R. Yuan, Y. Xiang, Programming cascaded recycling amplifications for highly sensitive and label-free electrochemical sensing of transcription factors in tumor cells, Biosens. Bioelectron. (2019) 111574.
[4] E. Schallmeiner, E. Oksanen, U. Stenman, K. Pettersson, L. Spångberg, U. Landegren, O. Ericsson, S. Eriksson, F. Medicinska, O.F.V. Medicinska, F.G.O.P. Institutionen, U. Uppsala, Sensitive protein detection via triple-binder proximity ligation assays, Nat. Methods 2 (2007) 135–137.
[5] R.K. Sharma, M. Otsuka, G. Gaba, S. Mehta, Inhibitors of transcription factor nuclear factor-kappa beta (NF-κβ)-DNA binding, RSC Adv. 5 (2013) 1282–1296.
[6] J.E. Darnell, Transcription factors as targets for cancer therapy, Nat. Rev. Canc. 10 (2002) 740–749.
[7] M.S. Hayden, S. Ghosh, Shared principles in NF-κB signaling, Cell 3 (2008) 344–362.
[8] A.C. Abraham, S.A. Shah, M. Golman, L. Song, X. Li, I. Kurtaliaj, M. Akbar, N.L. Millar, Y. Abu-Amer, L.M. Galatz, S. Thomopoulos, Targeting the NF-κB signaling pathway in chronic tendon disease, Sci. Transl. Med. 481 (2019) v4319.
[9] G.E. Griffin, K. Leung, T.M. Folks, S. Kunkel, G.J. Nabel, Activation of HIV gene expression during monocyte differentiation byinduction of NF-kB, Nature 6219 (1989) 70–73.
[10] F. Christian, E. Smith, R. Carmody, The regulation of NF-κB subunits by phosphorylation, Cells-Basel 1 (2016) 12.
[11] H. Ni, M. Ergin, Q. Huang, J. Qin, H.M. Amin, R.L. Martinez, S. Saeed, K. Barton, S. Alkan, Analysis of expression of nuclear factor kappaB (NF-kappaB) in multiple myeloma: downregulation of NF-kappaB induces apoptosis, Br. J. Haematol. 2 (2001) 279–286.
[12] A. Oeckinghaus, M.S. Hayden, S. Ghosh, Crosstalk in NF-κB signaling pathways, Nat. Immunol. 8 (2011) 695–708.
[13] K.R. Aupperle, B.L. Bennett, D.L. Boyle, P.P. Tak, A.M. Manning, G.S. Firestein, NF-kappa B regulation by I kappa B kinase in primary fibroblast-like synoviocytes, J. Immunol. 1 (1999) 427–433.
[14] Q. Zhang, M.J. Lenardo, D. Baltimore, 30 Years of NF-κB: a blossoming of relevance to human pathobiology, Cell 1–2 (2017) 37–57.
[15] H. Sui, L. Zhou, Y. Zhang, J. Huang, X. Liu, Q. Ji, X. Fu, H. Wen, Z. Chen, W. Deng, H. Zhu, Q. Li, Evodiamine suppresses ABCG2 mediated drug resistance by inhibiting p50/p65 NF-κB pathway in colorectal cancer, J. Cell. Biochem. 6 (2016) 1471–1481.
[16] O.A. Harari, J.K. Liao, NF-κB and innate immunity in ischemic stroke, Ann Ny Acad Sci 1 (2010) 32–40.
[17] B. Li, S. Xie, A. Xia, T. Suo, H. Huang, X. Zhang, Y. Chen, X. Zhou, Recent advance in the sensing of biomarker transcription factors, Trac. Trends Anal. Chem. (2020) 116039.
[18] M. Vitiello, M. Galdiero, E. Finamore, S. Galdiero, M. Galdiero, NF-κB as a potential therapeutic target in microbial diseases, Mol. Biosyst. 4 (2012) 1108.
[19] J. Yin, P. Gan, F. Zhou, J. Wang, Sensitive detection of transcription factors using near-infrared fluorescent solid-phase rolling circle amplification, Anal. Chem. 5 (2014) 2572–2579.
[20] Y. Zhang, F. Ma, B. Tang, C. Zhang, Recent advances in transcription factor assays in vitro, Chem. Commun. 26 (2016) 4739–4748.
[21] Y. Zhang, Q. Li, D. Xiang, K. Zhou, Q. Xu, C. Zhang, Development of a bidirectional isothermal amplification strategy for the sensitive detection of transcription factors in cancer cells, Chem. Commun. 63 (2020) 8952–8955.
[22] K. Zhang, Z. Fan, H. Li, J. Zhao, M. Xie, Determination of the concentration of transcription factor by using exonuclease III-aided amplification and gold nanoparticle mediated fluorescence intensity: a new method for gene transcription related enzyme detection, Anal. Chim. Acta (2020) 132–139.
[23] J. Ma, L. Xue, M. Zhang, C. Li, Y. Xiang, P. Liu, G. Li, An electrochemical sensor for Oct4 detection in human tissue based on target-induced steric hindrance effect on a tetrahedral DNA nanostructure, Biosens. Bioelectron. (2019) 194–199.
[24] E. Pazos, M. Garcia-Algar, C. Penas, M. Nazarenus, A. Torruella, N. Pazos-Perez, L. Guerrini, M.E. Vázquez, E. Garcia-Rico, J.L. Mascareñas, R.A. Alvarez-Puebla, Surface-enhanced Raman scattering surface selection rules for the proteomic liquid biopsy in real samples: efficient detection of the oncoprotein c-MYC, J. Am. Chem. Soc. 43 (2016) 14206–14209.
[25] Y. Chen, X. Yan, W. Yang, J. Wang, Q. Lu, B. Li, W. Zhu, X. Zhou, A signal transduction approach for multiplexed detection of transcription factors by integrating DNA nanotechnology, multi-channeled isothermal amplification, and chromatography, J. Chromatogr. A (2020) 461148.
[26] B. Li, Y. Chen, J. Wang, Q. Lu, W. Zhu, J. Luo, J. Hong, X. Zhou, Detecting transcription factors with allosteric DNA-Silver nanocluster switches, Anal. Chim. Acta (2019) 168–177.
[27] B. Li, Y. Chen, J. Wang, Q. Lu, W. Zhu, L. Xu, X. Shen, J. Luo, C. Zhu, X. Li, J. Hong, X. Zhou, DNA-silver nanoclusters/polypyrrole nanoparticles: a label-free and enzyme-free platform for multiplexed transcription factors detection, Sensor. Actuator. B Chem. (2018) 481–490.
[28] B. Li, L. Xu, Y. Chen, W. Zhu, X. Shen, C. Zhu, J. Luo, X. Li, J. Hong, X. Zhou, Sensitive and label-free fluorescent detection of transcription factors based on DNA-Ag nanoclusters molecular beacons and exonuclease III-assisted signal amplification, Anal. Chem. 14 (2017) 7316–7323.
[29] J.S. Chen, J.A. Doudna, The chemistry of Cas9 and its CRISPR colleagues, Nat Rev Chem 10 (2017) 78.
[30] J.S. Gootenberg, O.O. Abudayyeh, J.W. Lee, P. Essletzbichler, A.J. Dy, J. Joung, V. Verdine, N. Donghia, N.M. Daringer, C.A. Freije, C. Myhrvold, R.P. Bhattacharyya, J. Livny, A. Regev, E.V. Koonin, D.T. Hung, P.C. Sabeti, J.J. Collins, F. Zhang, Nucleic acid detection with CRISPR-Cas13a/C2c2, Science 6336 (2017) 438–442.
[31] R. Wang, X. Zhao, X. Chen, X. Qiu, G. Qing, H. Zhang, L. Zhang, X. Hu, Z. He, D. Zhong, Y. Wang, Y. Luo, Rolling circular amplification (RCA)-Assisted CRISPR/Cas9 cleavage (RACE) for highly specific detection of multiple extracellular vesicle MicroRNAs, Anal. Chem. 2 (2020) 2176–2185.
[32] J.S. Gootenberg, O.O. Abudayyeh, M.J. Kellner, J. Joung, J.J. Collins, F. Zhang, Multiplexed and portable nucleic acid detection platform with Cas13, Cas12a, and Csm6, Science 6387 (2018) 439–444.
[33] Y. Li, S. Li, J. Wang, G. Liu, CRISPR/Cas systems towards next-generation biosensing, Trends Biotechnol. 7 (2019) 730–743.
[34] Y. Chen, S. Yang, S. Peng, W. Li, F. Wu, Q. Yao, F. Wang, X. Weng, X. Zhou, N1-Methyladenosine detection with CRISPR-Cas13a/C2c2, Chem. Sci. 10 (2019) 2975–2979.
[35] M. Liang, Z. Li, W. Wang, J. Liu, L. Liu, G. Zhu, L. Karthik, M. Wang, K. Wang, Z. Wang, J. Yu, Y. Shuai, J. Yu, L. Zhang, Z. Yang, C. Li, Q. Zhang, T. Shi, L. Zhou, F. Xie, H. Dai, X. Liu, J. Zhang, G. Liu, Y. Zhuo, B. Zhang, C. Liu, S. Li, X. Xia, Y. Tong, Y. Liu, G. Alterovitz, G. Tan, L. Zhang, A CRISPR-Cas12a-derived biosensing platform for the highly sensitive detection of diverse small molecules, Nat. Commun. 1 (2019).
[36] Y. Xiong, J. Zhang, Z. Yang, Q. Mou, Y. Ma, Y. Xiong, Y. Lu, Functional DNA

regulated CRISPR-cas12a sensors for point-of-care diagnostics of non-nucleic-acid targets, J. Am. Chem. Soc. 1 (2019) 207–213.
[37] M. Zang, H. Su, L. Lu, F. Li, A split G-quadruplex-specific dinuclear Ir(III) complex for label-free luminescent detection of transcription factor, Talanta (2019) 259–266.
[38] S. Ranallo, M. Rossetti, K.W. Plaxco, A. Vallée-Bélisle, F. Ricci, A modular, DNA-based beacon for single-step fluorescence detection of antibodies and other proteins, Angew. Chem. Int. Ed. 45 (2015) 13214–13218.
[39] J. Wang, Exonuclease III protection assay with FRET probe for detecting DNA-binding proteins, Nucleic Acids Res. 2 (2005) e23.
[40] Y. Zhang, J. Hu, C. Zhang, Sensitive detection of transcription factors by isothermal exponential amplification-based colorimetric assay, Anal. Chem. 21 (2012) 9544–9549.
[41] J.S. Chen, E. Ma, L.B. Harrington, M. Da Costa, X. Tian, J.M. Palefsky, J.A. Doudna, CRISPR-Cas12a target binding unleashes indiscriminate single-stranded DNase activity, Science 6387 (2018) 436–439.
[42] S. Henikoff, Unidirectional digestion with exonuclease III creates targeted breakpoints for DNA sequencing, Gene 3 (1984) 351–359.
[43] C. He, J. Liu, Q. Zhang, C. Wu, A novel stable amperometric glucose biosensor based on the adsorption of glucose oxidase on poly(methyl methacrylate)–bovine serum albumin core–shell nanoparticles, Sensor. Actuator. B Chem. (2012) 802–808.
[44] V. Lonshakova-Mukina, E. Esimbekova, V. Kratasyuk, Impact of enzyme stabilizers on the characteristics of biomodules for bioluminescent biosensors, Sensor. Actuator. B Chem. (2015) 244–247.
[45] I. Fonfara, H. Richter, M. Bratovič, A. Le Rhun, E. Charpentier, The CRISPR-associated DNA-cleaving enzyme Cpf1 also processes precursor CRISPR RNA, Nature 7600 (2016) 517–521.
[46] B. Li, A. Xia, S. Zhang, T. Suo, Y. Ma, H. Huang, X. Zhang, Y. Chen, X. Zhou, A CRISPR-derived biosensor for the sensitive detection of transcription factors based on the target-induced inhibition of Cas12a activation, Biosens. Bioelectron. (2021) 112619.
[47] L. Lu, H. Su, F. Li, Ultrasensitive homogeneous electrochemical detection of transcription factor by coupled isothermal cleavage reaction and cycling amplification based on exonuclease III, Anal. Chem. 16 (2017) 8328–8334.
[48] K. Zhang, K. Wang, X. Zhu, M. Xie, Sensitive detection of transcription factors in cell nuclear extracts by using a molecular beacons based amplification strategy, Biosens. Bioelectron. (2016) 264–269.
[49] D. Zhu, L. Wang, X. Xu, W. Jiang, Colocalization recognition-activated cascade signal amplification strategy for ultrasensitive detection of transcription factors, Biosens. Bioelectron. (2017) 978–983.
[50] J. Ming, T. Jiang, Y. Wang, Z. Lv, Amplified detection of nuclear factor-kappa B activity and inhibition based on exonuclease III assisted cleavage-induced DNAzyme releasing strategy, Sensor. Actuator. B Chem. (2016) 605–611.
[51] F. Ma, Y. Yang, C. Zhang, Ultrasensitive detection of transcription factors using transcription-mediated isothermally exponential amplification-induced chemiluminescence, Anal. Chem. 12 (2014) 6006–6011.
[52] D. Zhu, L. Wang, X. Xu, W. Jiang, Label-free and enzyme-free detection of transcription factors with graphene oxide fluorescence switch-based multifunctional G-quadruplex-hairpin probe, Biosens. Bioelectron. (2016) 155–160.
[53] J. Liu, X. Song, Y. Wang, G. Chen, H. Yang, A graphene oxide (GO)-based molecular beacon for DNA-binding transcription factor detection, Nanoscale 12 (2012) 3655.
[54] V. De Simone, E. Franzè, G. Ronchetti, A. Colantoni, M.C. Fantini, D. Di Fusco, G.S. Sica, P. Sileri, T.T. MacDonald, F. Pallone, G. Monteleone, C. Stolfi, Th17-type cytokines, IL-6 and TNF-α synergistically activate STAT3 and NF-kB to promote colorectal cancer cell growth, Oncogene 27 (2015) 3493–3503.
[55] G. Pedersen, L. Andresen, M.W. Matthiessen, J. Rask-Madsen, J. Brynskov, Expression of Toll-like receptor 9 and response to bacterial CpG oligodeoxynucleotides in human intestinal epithelium*, Clin. Exp. Immunol. 2 (2005) 298–306.
[56] Z. Huang, D. Tian, Y. Liu, Z. Lin, C.J. Lyon, W. Lai, D. Fusco, A. Drouin, X. Yin, T. Hu, B. Ning, Ultra-sensitive and high-throughput CRISPR-p owered COVID-19 diagnosis, Biosens. Bioelectron. (2020) 112316.
[57] S. Safe, J. Abbruzzese, M. Abdelrahim, E. Hedrick, Specificity protein transcription factors and cancer: opportunities for drug development, Canc. Prev. Res. 7 (2018) 371–382.
[58] K. Taniguchi, M. Karin, NF-κB, inflammation, immunity and cancer: coming of age, Nat. Rev. Immunol. 5 (2018) 309–324.
[59] C. Leung, S.P. Grill, W. Lam, Q. Han, H. Sun, Y. Cheng, Novel mechanism of inhibition of nuclear factor-κb DNA-binding activity by diterpenoids isolated fromIsodon rubescens, Mol. Pharmacol. 2 (2005) 286–297.
[60] X. Dong, F. Liu, M. Li, Inhibition of nuclear factor κB transcription activity drives a synergistic effect of cisplatin and oridonin on HepG2 human hepatocellular carcinoma cells, Anti Canc. Drugs 4 (2016) 286–299.